# DETERMINATION OF THE NORMAL COMPONENT OF INDUCED VELOCITY IN THE FLOW-FIELD ABOUT A TWO-BLADED ROTOR HOVERING IN GROUND EFFECT

A THESIS

Presented to

the Faculty of the Graduate Division

by

Austin K. Veatch, Jr.

In Partial Fulfillment

of the Requirements for the Degree

Master of Science in Aeronautical Engineering

Georgia Institute of Technology

May, 1960

"In presenting the dissertation as a partial fulfillment of the requirements for an advanced degree from the Georgia Institute of Technology, I agree that the Library of the Institution shall make it available for inspection and circulation in accordance with its regulations governing materials of this type. I agree that permission to copy from, or to publish from, this dissertation may be granted by the professor under whose direction it was written, or, in his absence, by the dean of the Graduate Division when such copying or publication is solely for scholarly purposes and does not involve potential financial gain. It is understood that any copying from, or publication of, this dissertation which involves potential financial gain will not be allowed without written permission.

_____

_____"

DETERMINATION OF THE NORMAL COMPONENT OF INDUCED VELOCITY IN THE FLOW-FIELD ABOUT A TWO-BLADED ROTOR HOVERING IN GROUND EFFECT

Approved:

Walter Castles, Jr.

Robin B. Gray

Thomas W. Jackson

Date Approved by Chairman: June 2, 1960

## ACKNOWLEDGEMENTS

I wish to express my sincere appreciation to Professor Walter Castles, Jr., for the guidance rendered me in the preparation of this thesis. I also want to thank Doctor Robin B. Gray and Doctor Thomas W. Jackson for their review and comments.

# TABLE OF CONTENTS

# LIST OF FIGURES

Figure Page

# LIST OF SYMBOLS

| | |
|---|---|
| A | area of the rotor disc |
| B | magnetic flux density |
| b | number of blades of rotor |
| $C_T$ | rotor thrust coefficient |
| h/R | nondimensional distance above tip path plane |
| MR | meter reading, decibels |
| N | subscript for a value at the reference point |
| n | number of turns of wire on reference coil |
| P | subscript for a value at an arbitrary point P |
| R | rotor radius |
| $R_c$ | radius of reference coil |
| $R_m$ | wire model rotor radius |
| r | radial distance from rotor axis |
| w | component of induced velocity normal to the rotor plane |
| Z/R | nondimensional distance of rotor above ground plane |
| $\Gamma$ | circulation strength |
| $\psi$ | azimuth angle of blade feathering axis measured from downwind position and in direction of blade rotation |
| $\rho$ | mass density |
| $\Omega$ | angular velocity of the rotor |

## SUMMARY

This paper presents the result of experiments conducted to determine the normal component of induced velocity in the flow-field of a two-bladed lifting rotor hovering at a height of one rotor radius above the ground. The information was obtained using the electromagnetic analogy developed in reference 1, in which a smoke technique was utilized to determine the tip vortex geometry for a two-bladed lifting rotor hovering at a height of one rotor radius. A wire model, built to simulate the tip vortex shed by one blade of the model rotor and a constant blade bound vortex, was used in the experiments for the current paper. The component of the magnetic field strength normal to the tip path plane was measured at various points about the model and its image. The measurements covered the region extending 0.4 rotor radius above and below the tip path plane and outward to 3.0 rotor radii. The measured components of magnetic field strength were converted to induced velocities nondimensionalized in terms of the rotor radius and the tip vortex strength.

The values obtained for the wake and its image were added by the principle of superposition to give a total nondimensional induced velocity for the vortex system of one

blade. Effects of the second vortex system were then evident from the system's symmetry and were included to give total values for the two-bladed rotor. The final results are given in graphical form and show the nondimensional normal component of induced velocity in five planes parallel to the tip path plane.

A method is presented for using the graphs to estimate downwash velocities on a helicopter fuselage and the interference induced velocities arising from a second two-bladed rotor mounted side-by-side or in tandem. A sample problem is worked out with the results shown graphically.

# CHAPTER 1

## INTRODUCTION

Many lifting rotor problems require a knowledge of the induced velocities in the vicinity of the rotor. These velocities are induced by the vortex system of the rotor itself and they are supplemented by the velocities induced by any other vortex system in the flow field. This study is concerned with the determination of the normal component of the induced velocity for a two-bladed rotor hovering in ground effect.

Most studies of the induced flow field about a rotor in ground effect assume that the rotor wake vortex distribution consists of a right circular vortex cylinder, made up of an infinite number of vortex rings of infinitesimal strength, extending from the tip path plane to the ground along with the image of the cylinder below the ground plane. This is not truly representative of the actual wake and it follows that a study of the induced velocity based on the actual wake vortex distribution should give better results. This study, therefore, utilized the hovering model of reference 1, in which a smoke technique was used to determine the actual tip vortex geometry for a two-bladed lifting rotor. An electromagnetic-analogy wire model, shown in figure 1,

was constructed from the smoke studies. The induced velocity at each point was calculated from a measurement of the magnetic field strength at that point in the vicinity of the wire model. In reference 1, induced velocities were given only for positions along the blade axes. The current report gives normal induced velocities in five planes at nondimensional distances from the tip-path plane of h/R = -0.4, -0.2, 0, 0.2, and 0.4, and extending outward three rotor radii.

Sample problems are included to demonstrate possible uses for the experimental data contained herein. A typical single-rotor helicopter was chosen for which downwash velocities over the fuselage were estimated. Also, a tandem-rotor helicopter was chosen and the approximate values of the nondimensional interference induced velocity determined over the disks of both rotors. The sample problems assume the flow from an isolated rotor may be superimposed upon objects in the flow field, such as the helicopter fuselage, or upon the flow from other rotors. This is not strictly valid since the geometry of the wake vortices would be influenced by objects in the flow field or the flow from other rotors. The method of superposition should, however, give a good first approximation.

# CHAPTER II

## APPARATUS AND EXPERIMENTAL PROCEDURE

The equipment used for the experimental portion of this thesis consisted of five basic components:

1. The primary coil (wire model of the tip vortex helix)
2. The reference coil
3. The secondary coil (search coil)
4. The amplifier and output meter
5. The power supply

This equipment was essentially the same as used for the experiments of reference 1, in which only the tip vortex was simulated, except that the wire lead-in was extended across the blade feathering axis to represent the blade bound vortex.

The basic components are described as follows:

Primary coil (tip vortex model).--As described in reference 1, the electromagnetic model was constructed from data obtained from a study of smoke pictures taken of a two-bladed, teetering type, four-foot diameter model rotor with zero coning angle. The blades had an NACA 43015 airfoil section, a square tip with a chord of 1.508 inches, a taper ratio of 2/1, and a solidity ratio of 0.05.

The structure supporting the wire vortex model was

made from fiberboard and plywood as shown in figure 1. No. 17, Brown and Sharpe gage, copper wire was used and wrapped upon the support to simulate the tip vortex helix. From the tip of the blade the wire was brought to the center of the tip path plane along the blade feathering axis and down through the axis of the rotor to the ground plane. Thus the measured values of the normal component of magnetic field strength included the effects of the wire simulating the blade bound vortex but not the effects of the wire along the rotor axis as it was always parallel to the axis of the search coil. The lead-in wires were placed in the ground plane and their contribution cancelled out by the superposition of the image which was derived from the same model. Outside the model the leads were connected to a twisted pair from the power supply. The wire vortex model had a simulated rotor radius of six inches, the tip path plane was six inches above the ground plane, and the wire helix spiraled downward and outward to a radius of eighteen inches.

Reference coil.--The reference coil consisted of nine closely spaced turns of No. 17 gage wire wrapped on a plexiglass ring. This coil was in series with the wire model and located far enough from the model so that it did not affect the results. The meter readings were referenced to the magnetic field strength at the center of this coil. The reference coil is shown in figure 2.

Search coil.--The search coil consisted of 1000 turns of

No. 40, Brown and Sharpe gage, copper wire wound on a plexiglass core mounted on a plexiglass support as shown in figure 3. The coil had a diameter of 0.35 inches to the center of the wire bundle which had a cross section approximately .09 inches square. A coaxial cable was used to connect the search coil to the amplifier.

Amplifier and output meter.--The pickup circuit included a commercial standing wave indicator in addition to the search coil and coaxial cable described above. This indicator, which had a maximum sensitivity of 0.1 microvolt, consisted of an indicating meter, a high-gain 400 cycle fixed-frequency amplifier with a calibrated gain control covering a 60 decibel range, and a narrow 400 cycle band-pass-filter network which had a sharp cutoff at 400 $\pm$ 5 cycles per second. The input impedance of the amplifier was 200,000 ohms, sufficient to eliminate any calibration of the meter scale. The amplifier was placed in a separate room from the field coils to eliminate any appreciable magnetic coupling from these coils. The standing wave indicator is shown in figure 4.

Power supply.--The power supply was a 400 cycle aircraft alternator driven by a synchronous motor. Other components in the circuit included a voltmeter, ammeter, variable resistors and capacitors. The resistors were adjusted to allow approximately 3 amperes current and the capacitors were adjusted to place the entire circuit in resonance. The

power supply system was in another room to minimize direct magnetic coupling. A schematic drawing of the system is shown in figure 5.

Field survey procedure.--The primary coil circuit was given a warm-up period of forty-five minutes prior to any surveys. The search coil was then positioned in the plane of, and coaxially with, the reference coil. The meter reading was then noted. For all subsequent measurements of the reference coil field strength the meter reading was adjusted to the original value using the calibration control. The magnetic field strength about the wire model was then measured at points along radial lines extending from the axis of the model out to three rotor radii. This was done for the angle $\psi$ = 0°, 45°, 90°, 135°, 270°, and 315° measured from a blade feathering axis in the $\psi$ = 0° position. The measurements were made in planes parallel to the tip path plane at h/R = -0.4, -0.2, 0.0, 0.2 and 0.4.

The effect of the ground plane was determined by the method of images, using the same model as the image. The model was raised from the table on wooden supports and measurements taken in planes below the tip path plane at distances of 1.6, 1.8, 2.0, 2.2 and 2.4 rotor radii. Thus the resultant normal component was found by taking the difference of the nondimensional normal induced velocity obtained from the first set of data and that value obtained from properly corresponding points in the second, or

"image," set.

During all experiments the search coil was frequently returned to the calibration position at the center of the reference coil.

Reduction of data.--The output meter was calibrated in decibels and it was necessary to convert the meter readings into equivalent values of the nondimensional normal component of induced velocity. This conversion was accomplished through the following formulas derived in reference 1:

$$\frac{B_P}{B_N} = \frac{\text{antilog } 0.1\ (MR)_P}{\text{antilog } 0.1\ (MR)_N}$$

$$\frac{wR}{\Gamma} = \frac{n}{2}\left(\frac{R_m}{R_c}\right)\frac{B_P}{B_N}$$

where

$B_P$ magnetic flux density at point under consideration

$B_N$ magnetic flux density at center of reference coil

MR meter reading, decibels

w component of tip-vortex induced velocity normal to the rotor disk

R rotor radius

n number of turns on reference coil

$R_m$ wire model rotor radius

$R_c$ radius of reference coil

The direction of the induced velocity w was

determined from the vortex geometry and a study of the trends in the experimental data.

After each meter reading was converted as described above, it was then possible to obtain the resultant normal component by superposition. The resultant contribution of the vortex system of one blade was found by taking the difference of the values obtained from the model and the values obtained from its image. An example is given in figure 6 (a), which shows the measurements made for the tip vortex and its image, and the resultant, for points along the 45° - 225° line at a height h/R of -0.4. In this example the blade is at $\psi = 0°$.

The symmetry of the hovering rotor allows us to add the effects of the vortex system of the second blade without further measurements. For example, the values obtained at $\psi = 45°$ for a single blade at $\psi = 0°$ are identical, by symmetry, to those obtained at $\psi = 225°$ for a single blade at $\psi = 180°$. Therefore we may add the values obtained at $\psi = 45°$ and $\psi = 225°$ for the vortex system of the single rotor blade to obtain the total normal induced velocity for the two-bladed rotor. This is illustrated in figure 6 (b).

# CHAPTER III

## RESULTS

Figures 7 (a) - 7 (e) show the nondimensional normal component of induced velocity, $wR/\Gamma$, that was associated with the vortex system, for the horizontal planes at nondimensional distances from the rotor plane of $h/R = -0.4$, $-0.2$, $0$, $0.2$, and $0.4$, respectively. These figures graphically present the results obtained for a two-bladed rotor hovering at a height of one rotor radius with the blades in the 0° - 180° position.

Because of the physical interference between the search coil and wire helix no measurements could be taken closer to a wire than approximately .05 R laterally and .015 R vertically. Values for points closer to the wire had to be evaluated by extrapolation.

In the plane of the rotor large changes occur in the normal component of induced velocity when surveying perpendicular to, and in close proximity with, the wire representing the blade feathering axis. Since such changes would actually be distributed over the blade chord, this region is deleted in figure 7 (c).

The results herein presented are exactly applicable only to rotors having the same vortex geometry as the

electromagnetic-analogy wire model used in the experiments. It is believed, however, that the results may be used with engineering accuracy for systems having thrust coefficients not appreciably different from the value of $C_T \approx .004$ measured for the model rotor in reference 1, on which the wire model was based. Figure 8 gives a comparison of the distribution of the normal component of induced velocity along the blade axis, as taken from the experimental results shown in figure 7 (c), with the mathematical results obtained by Knight and Hefner in reference 3. The curves compared are for approximately equal values of induced velocity at the blade thrust center.

# CHAPTER IV

## APPLICATION OF RESULTS

Estimation of mean downwash velocities over the fuselage of a typical two-bladed single rotor helicopter.--In many helicopter design problems it is necessary to estimate the local velocities on some portion of the aircraft. As an illustration of the use of the experimental data contained herein, it was assumed that a designer needed the downwash velocities on a helicopter fuselage located approximately 0.2 R below the plane of the rotor. For the purpose of this example a typical two-bladed single-rotor helicopter is assumed to be hovering with the rotor plane at a height of one rotor radius above the ground. The following pertinent data was assumed:

Weight = 2000 lbs.

Rotor radius, R = 20 ft.

Angular velocity of the rotor, $\Omega$ = 30 radians/sec.

In order to use the values of nondimensional induced velocity given in figure 7, the assumed constant blade circulation, $\Gamma$, for the sample helicopter was computed as follows:

$$C_T = \frac{W}{\frac{1}{2}\rho(\Omega R)^2 A} = \frac{2000}{\frac{1}{2}(.00238)(600)^2\pi(20)^2} = 0.00371$$

$$\Gamma = \frac{2\pi\Omega R^2 C_T}{b} = \frac{2\pi(30)(20)^2(.00371)}{2} = 140 \text{ ft}^2/\text{sec}$$

Figure 7 (b) was utilized to construct a plot of nondimensional induced velocity, $wR/\Gamma$, against azimuth angle for several distances from the hub, and the plots averaged by numerical integration. The plots, and the results of numerical integration, are shown in figure 9. The mean values of nondimensional induced velocity, $wR/\Gamma$, were multiplied by the factor $\Gamma/R$ to obtain mean downwash velocities which were then plotted against the rotor radius in figure 10.

Estimation of interference induced velocities in the plane of both rotors of a two-bladed tandem-rotor helicopter.--The data in figure 7 may be used to estimate the interference values of the normal component of induced velocity arising from the addition of a second rotor to the system. Although it is recognized that the wake vortex system of an isolated rotor is not exactly the same as that of a rotor in a tandem-rotor system, the technique of superposition was used as a first approximation for a sample problem.

For this sample problem the helicopter was assumed to be hovering with the rotors one rotor radius above the ground. The rotor axes are spaced two rotor radii apart and are operating 90° out of phase with each other. From an inspection of figure 7 it is obvious that the interference

normal induced velocities are time dependent and vary with the position of the blade axes. For a complete study it would be necessary to analyze the system for all azimuth angles of the rotor blades. For this example the interference normal induced velocities will be determined only for the situation where the blades of one rotor are in the 0° - 180° position and the blades of the other are in the 90° - 270° position. The general configuration is shown in figure 8.

The interference velocities are determined by constructing circles representing the second rotor disk in the proper geometric position on figure 7 (c) and reading the nondimensional normal component directly at the desired radial and azimuth coordinates within the inscribed circle. This is illustrated by figures 11 and 12, wherein the induced velocities for two points at .75 R on the blade axes, as shown in figure 11, are located in figure 12. It should be noted that the position of the inscribed circle will rotate around the central axis as the phase angle of the blades change.

# CHAPTER V

## CONCLUSIONS

It is believed that the experimental results contained herein are of engineering accuracy when used for two-bladed rotor systems having thrust coefficients not appreciably different from the value of $C_T \approx .004$ measured for the model rotor in reference 1, on which the wire model was based. The helical wire wake-vortex model used should produce more realistic results than are obtained by studies in which a cylindrical wake is assumed.

The values of the nondimensional normal component of induced velocity, $wR/\Gamma$, given in figure 7 should be useful for estimating local velocities in the flow field of a two-bladed rotor hovering at approximately one rotor radius above the ground. A sample problem is given in which the downwash velocities on the fuselage are estimated for a typical two-bladed single-rotor helicopter. In a second sample problem a method is given for estimating the interference induced velocity over the rotor disks of a two-bladed tandem-rotor helicopter.

# FIGURES

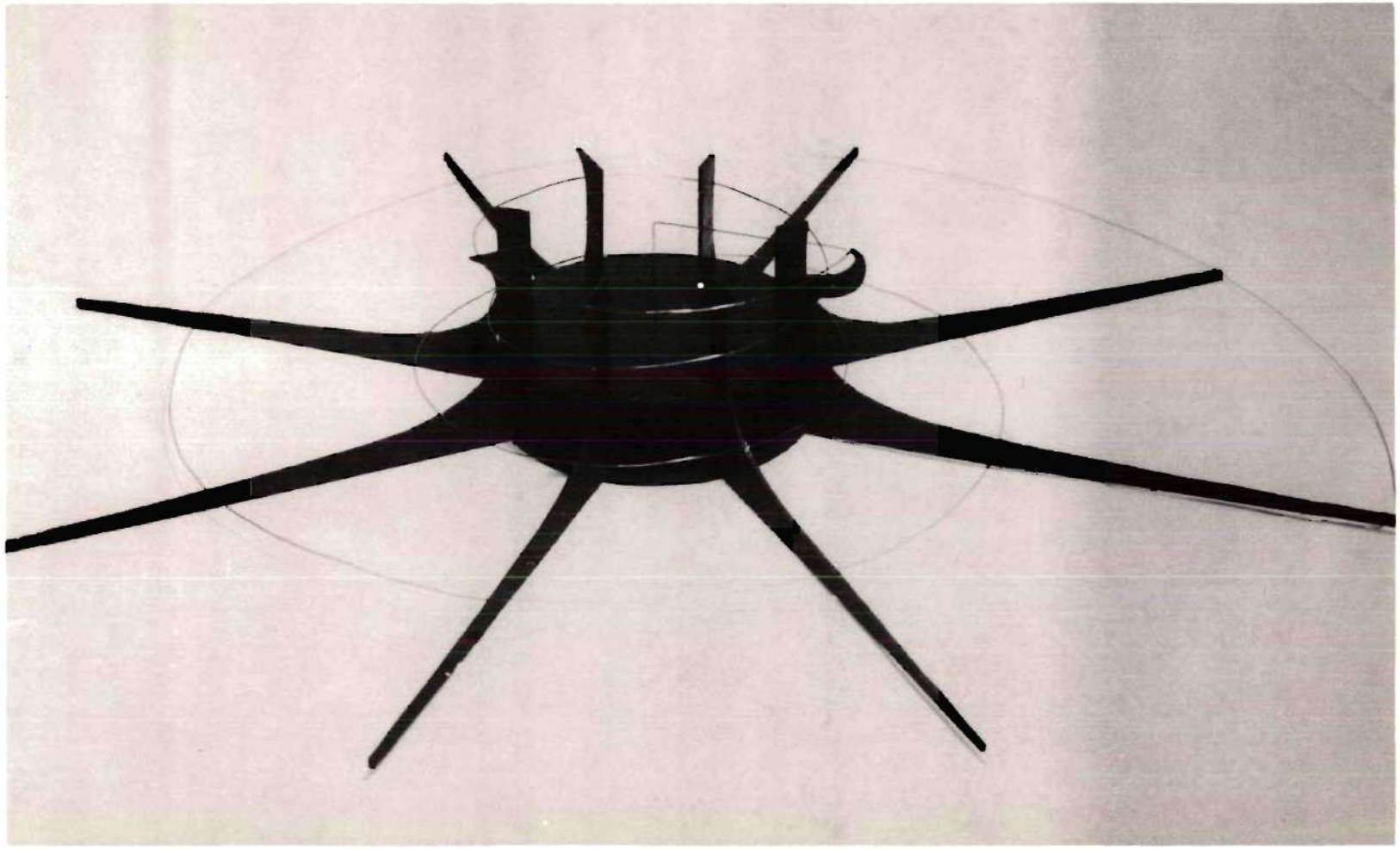

Figure 1. Electromagnetic Analog of One Tip Vortex of a Two-Bladed Model Rotor Hovering at Z/R = 1.0

Figure 2. Reference Coil

Figure 3. Search Coil


Figure 4. Amplifier and Indicator Unit

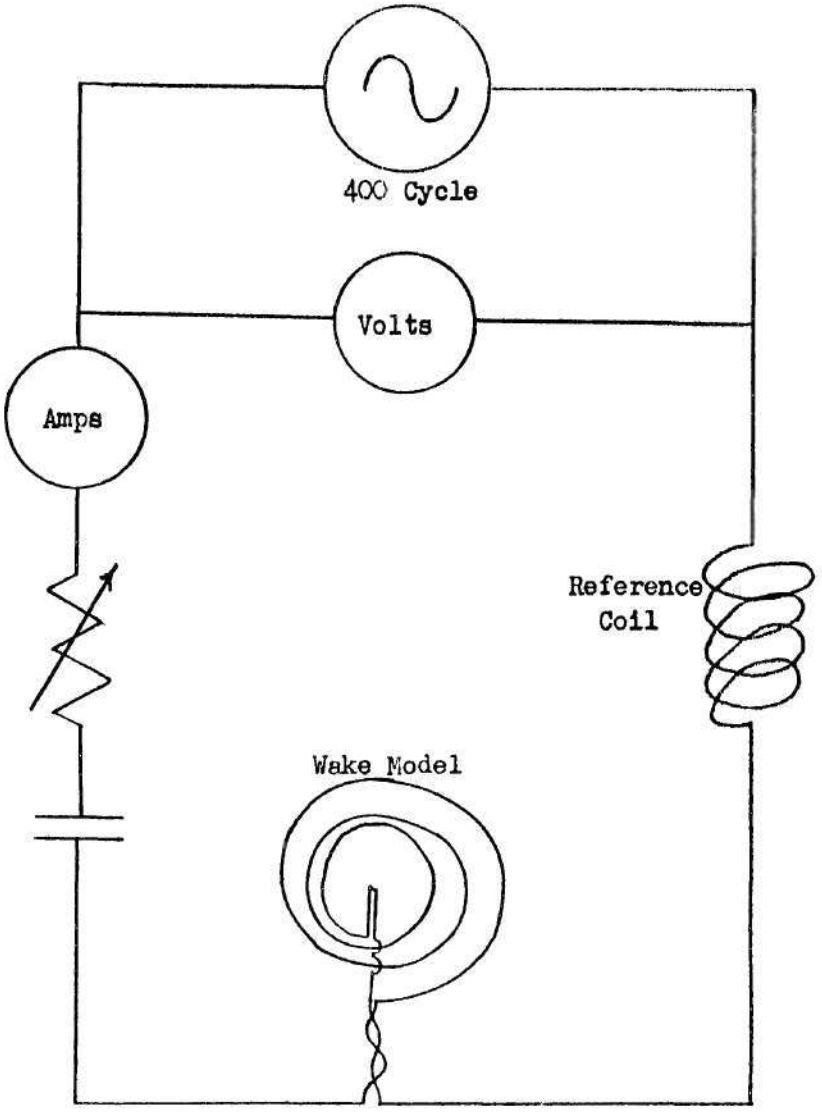


Figure 5. Schematic of the Power Supply System

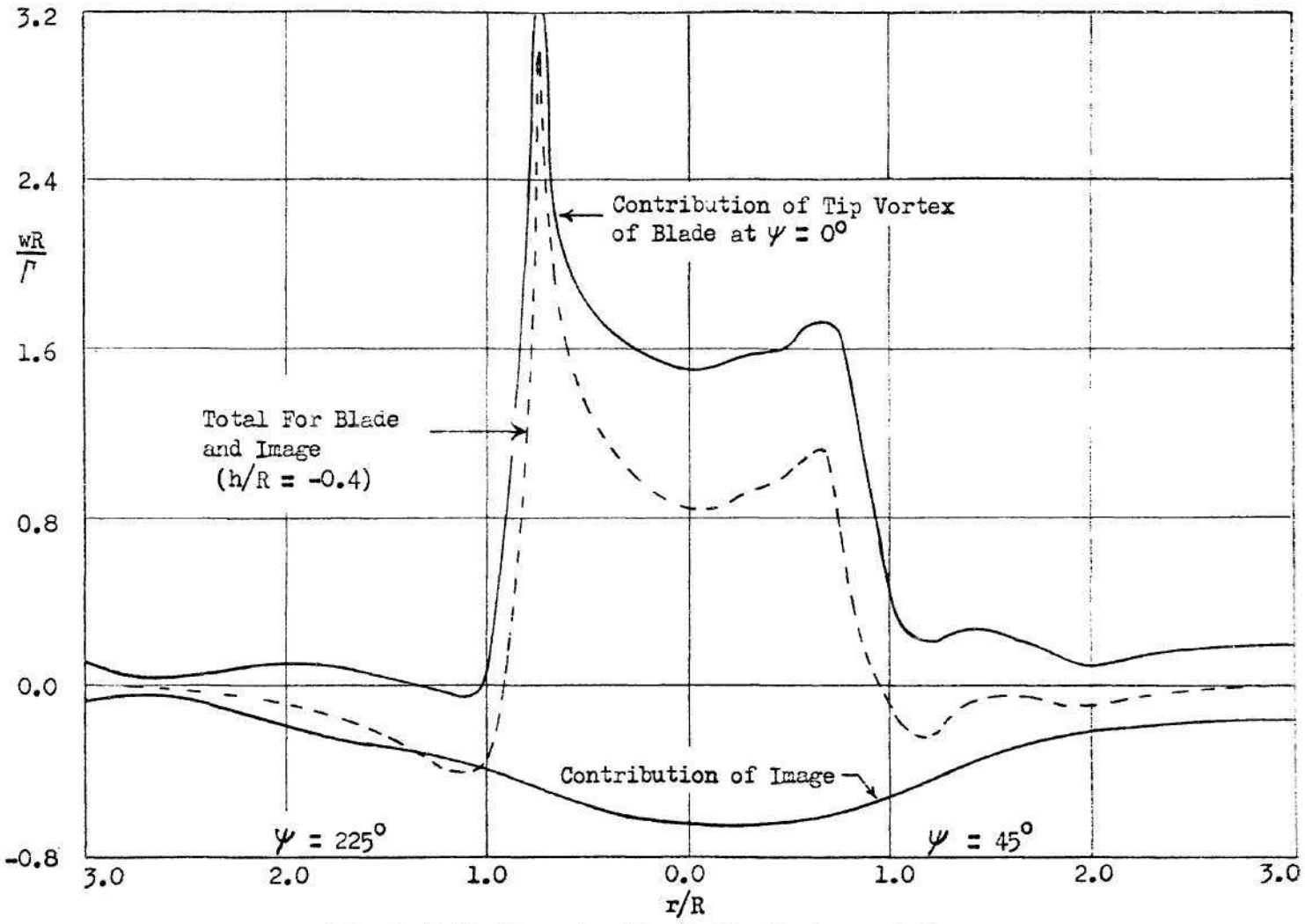


(a) Contribution of a Single Tip Vortex and its Image

Figure 6. Typical Plot of Nondimensional Normal Component of Induced Velocity

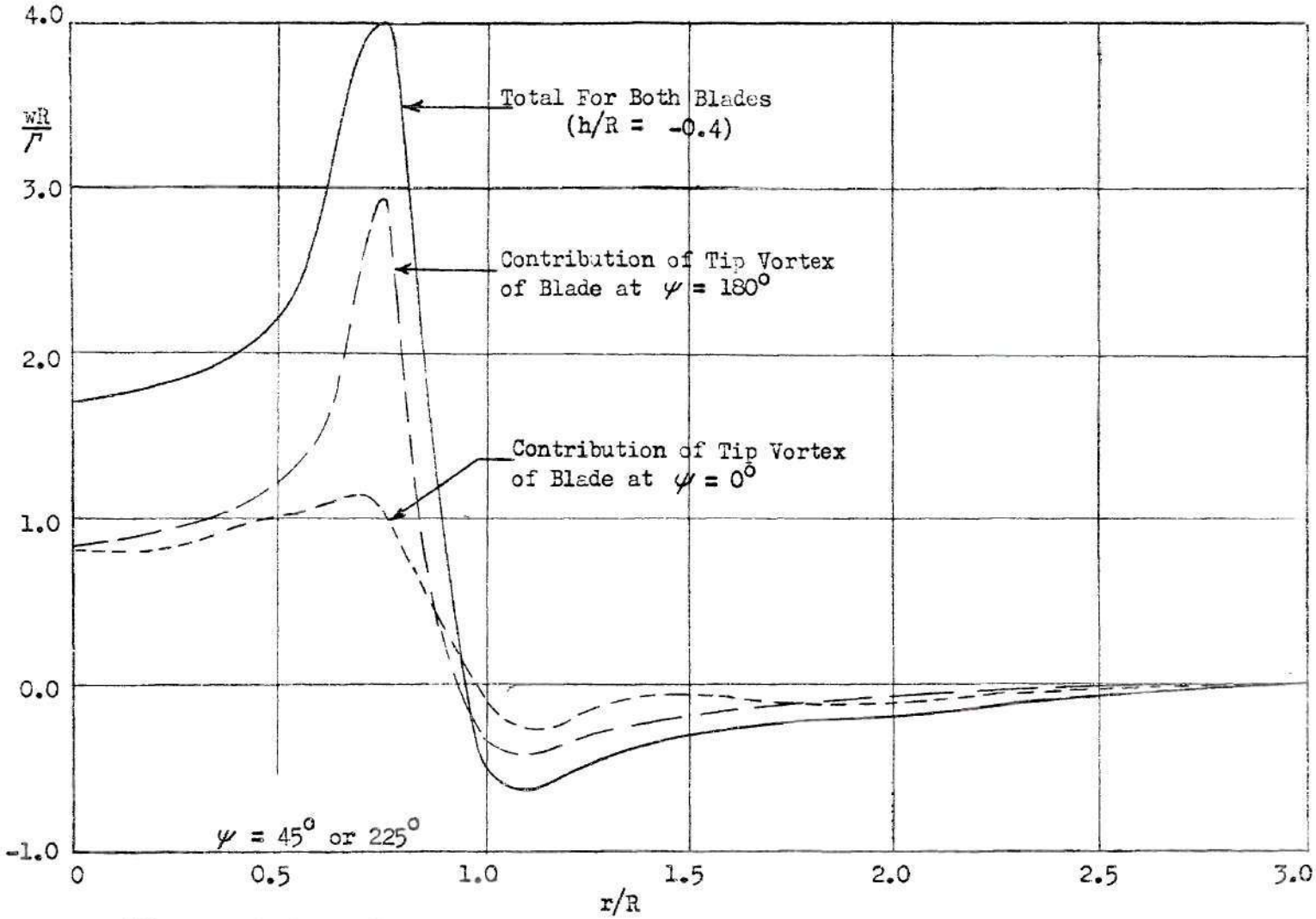


(b) Resultant Found By Superposition of the Second Tip Vortex Contribution

Figure 6. Continued

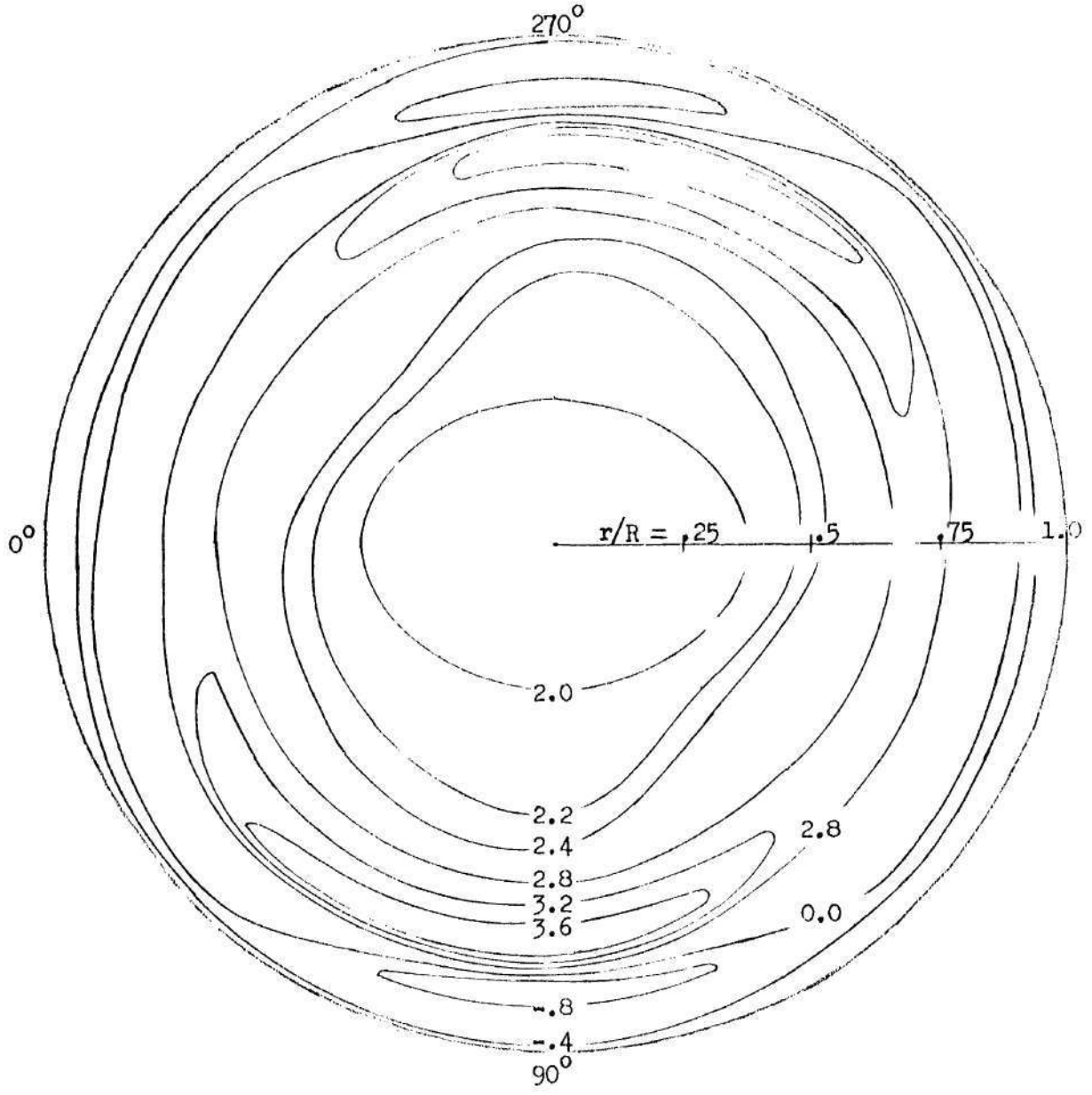


(a) For Nondimensional Distance From Tip Path Plane h/R = -0.4

Figure 7. Variation of Nondimensional Normal Component of Induced Velocity

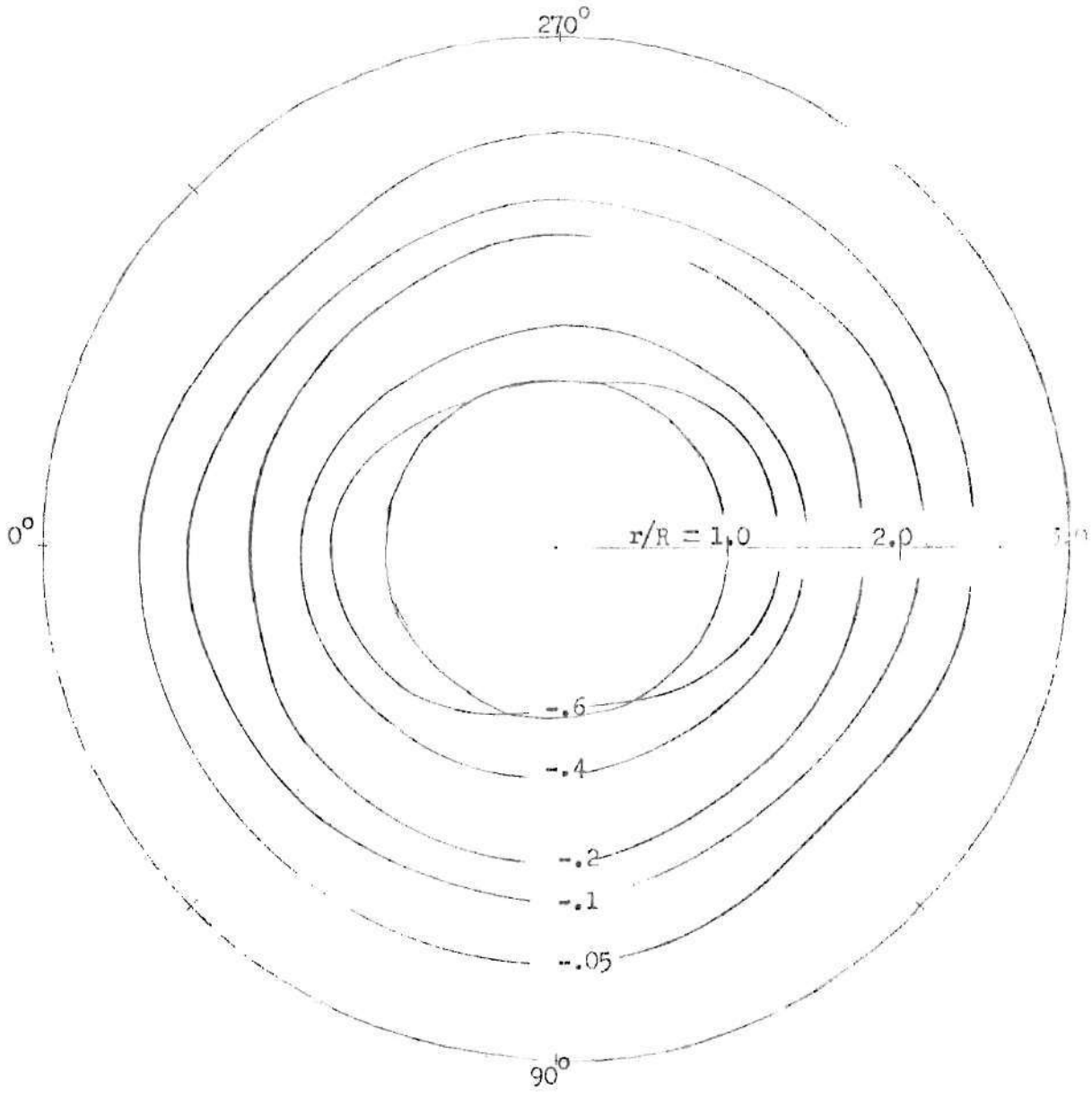


Figure 7(a). Continued

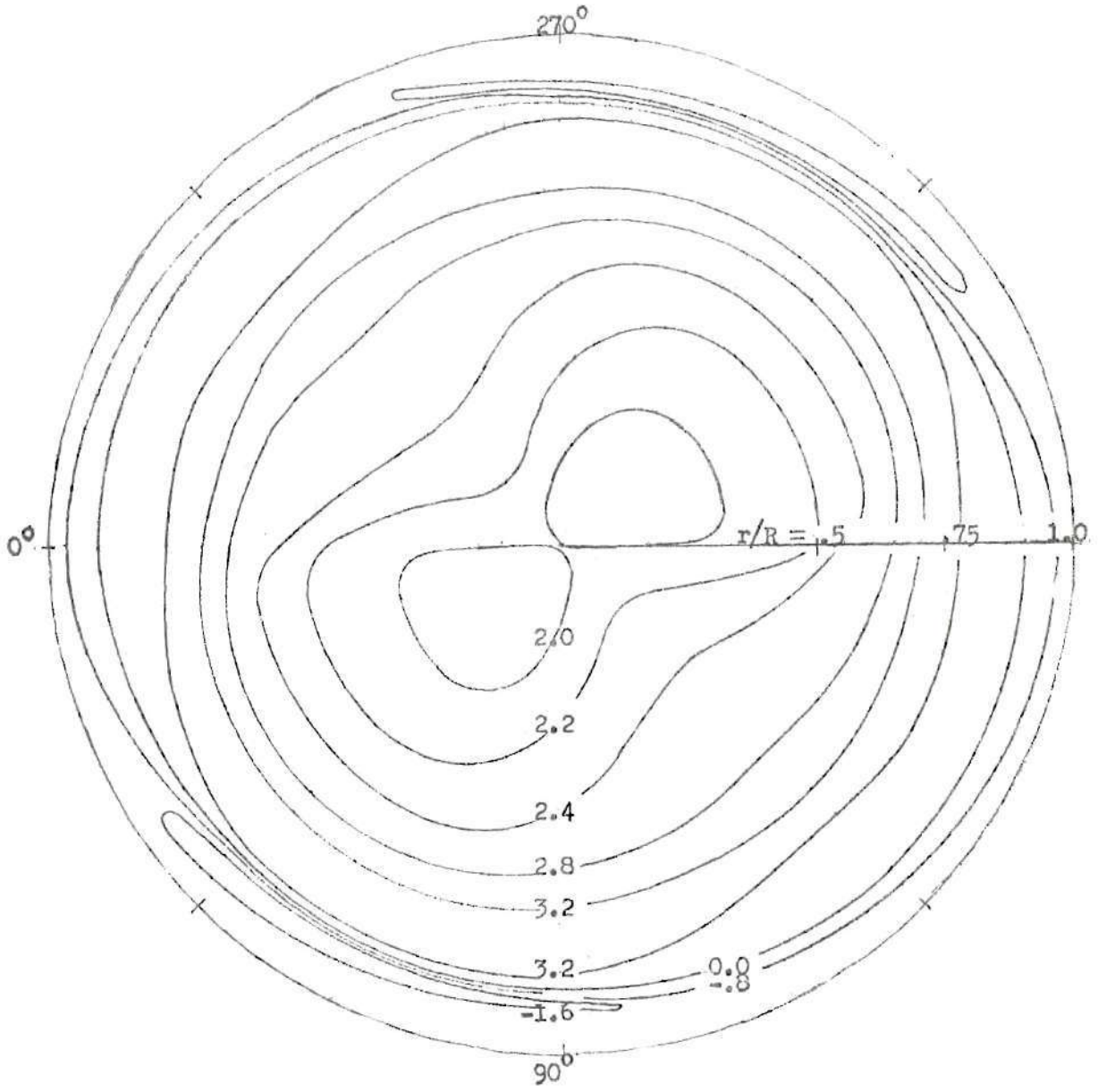


(b) For Nondimensional Distance From Tip Path Plane h/R = -0.2

Figure 7. Continued

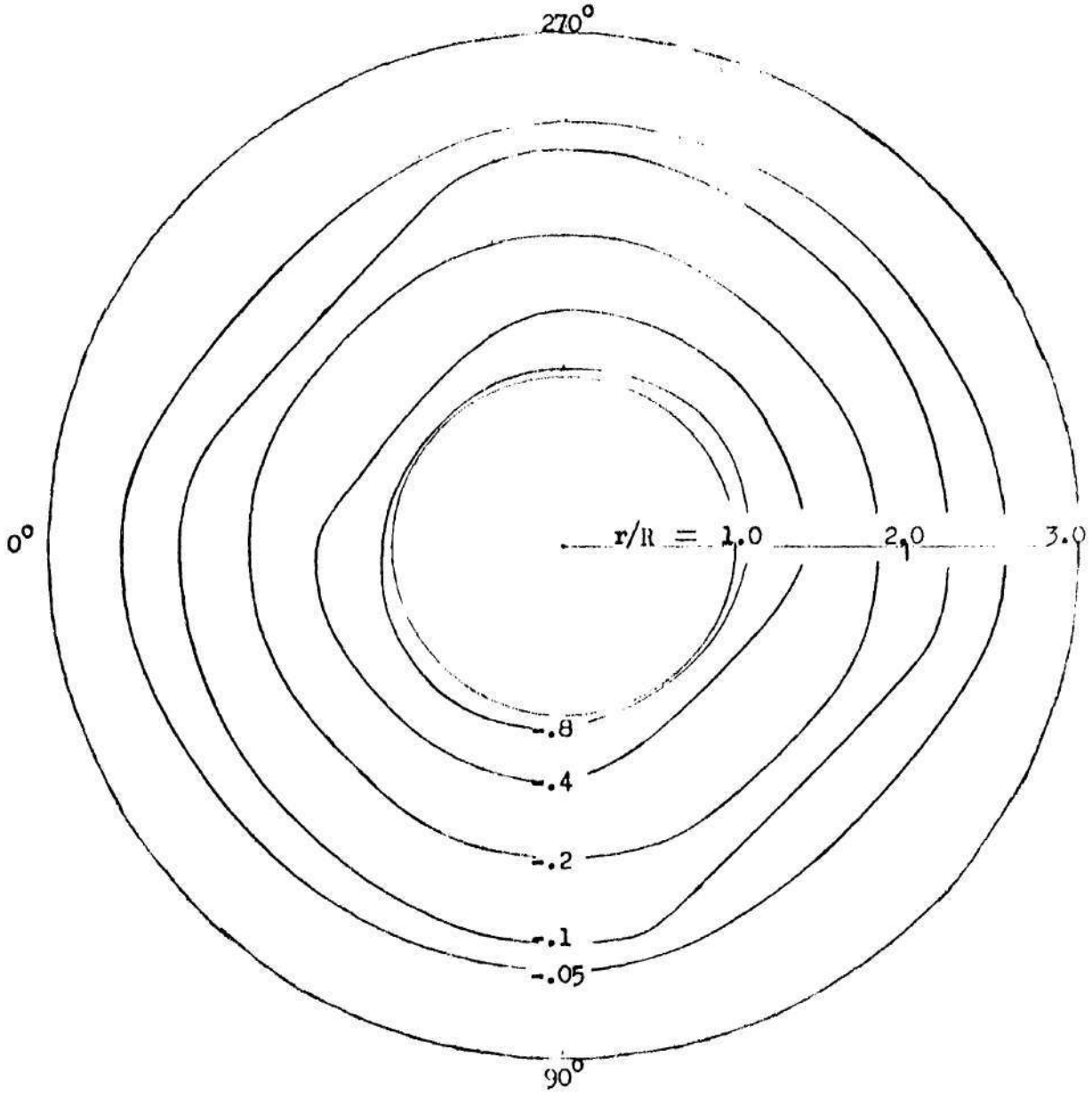


Figure 7(b). Continued

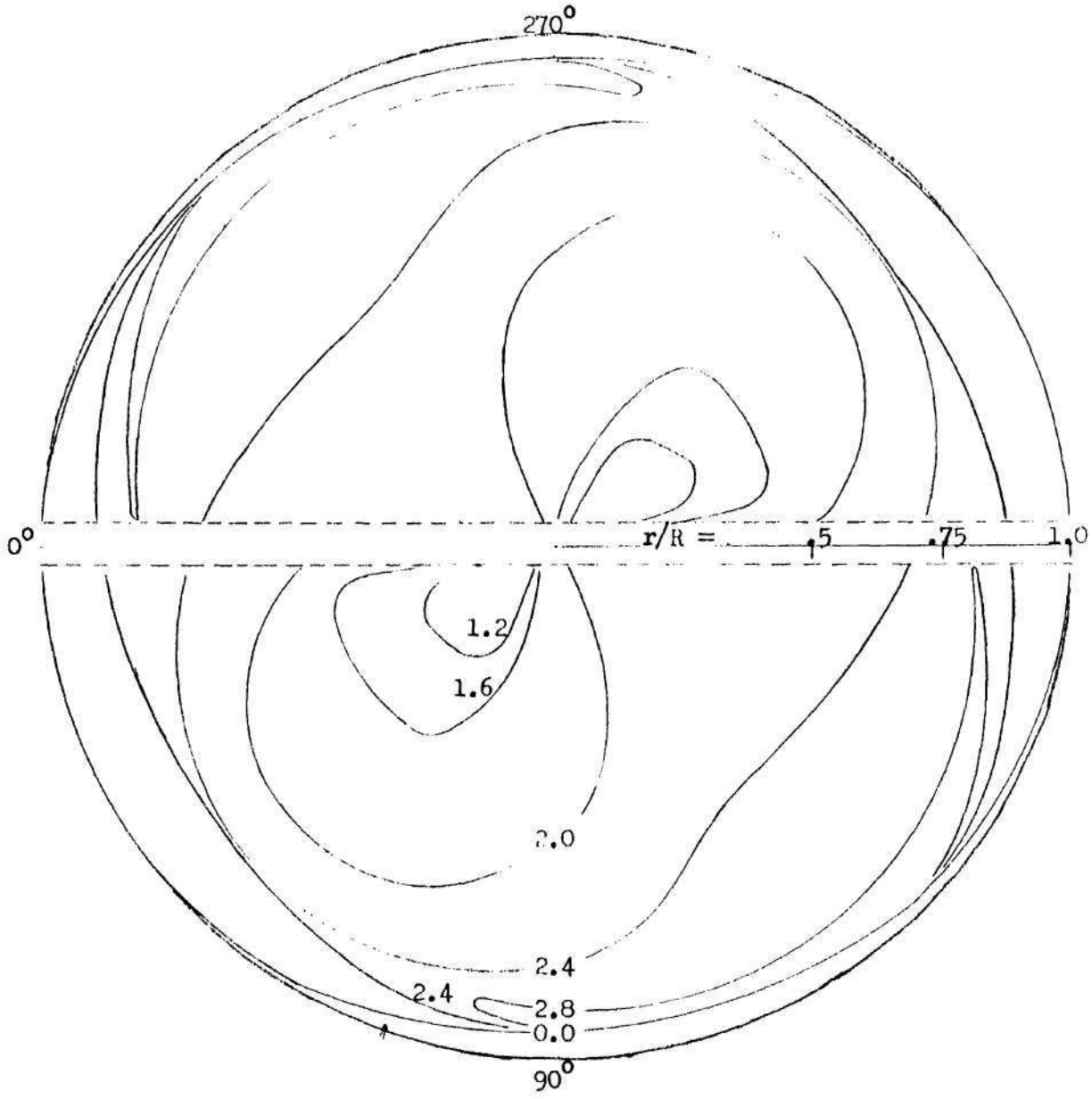


(c) For Nondimensional Distance From Tip Path Plane h/R = 0.0

Figure 7. Continued

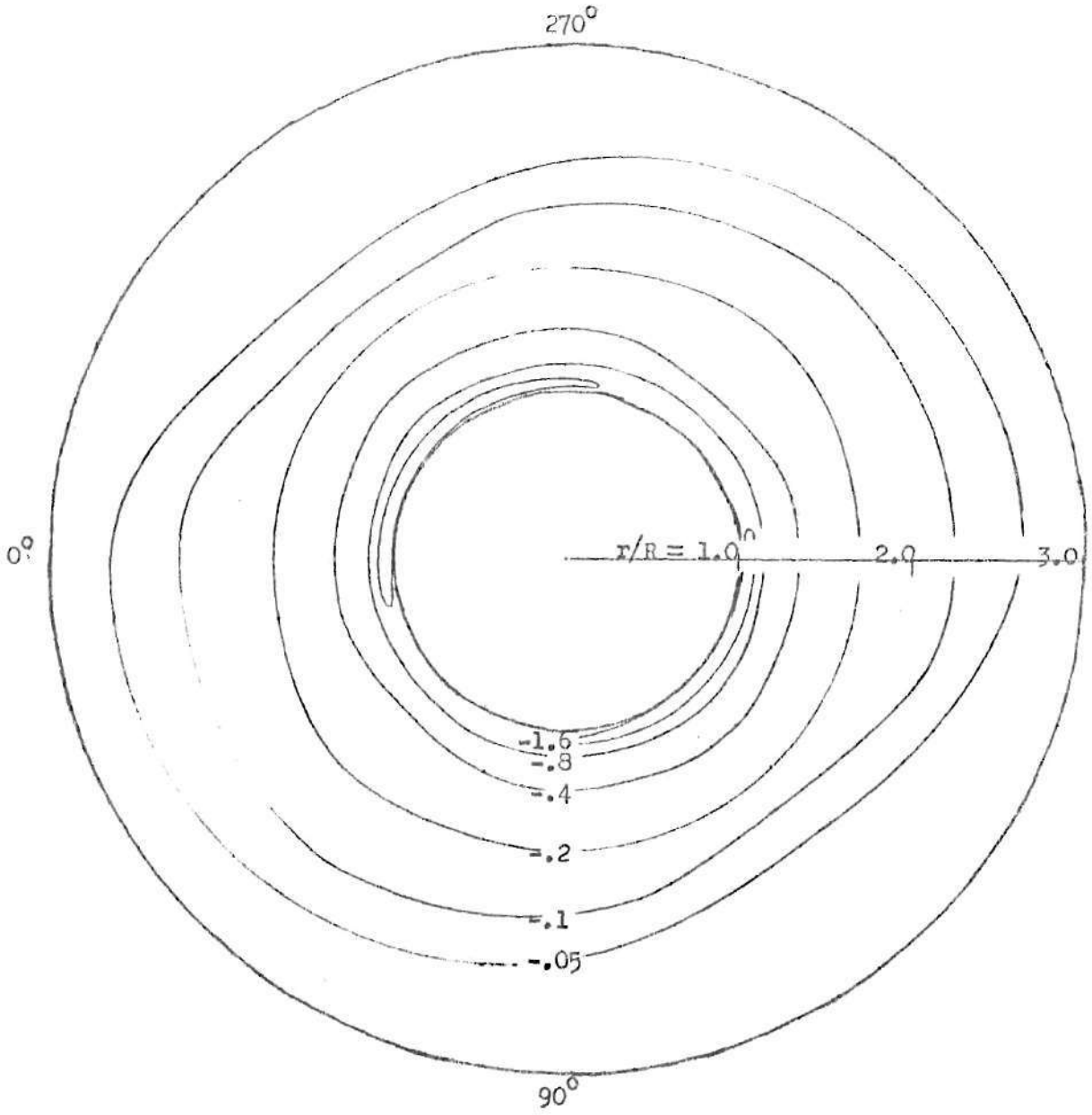


Figure 7(c). Continued

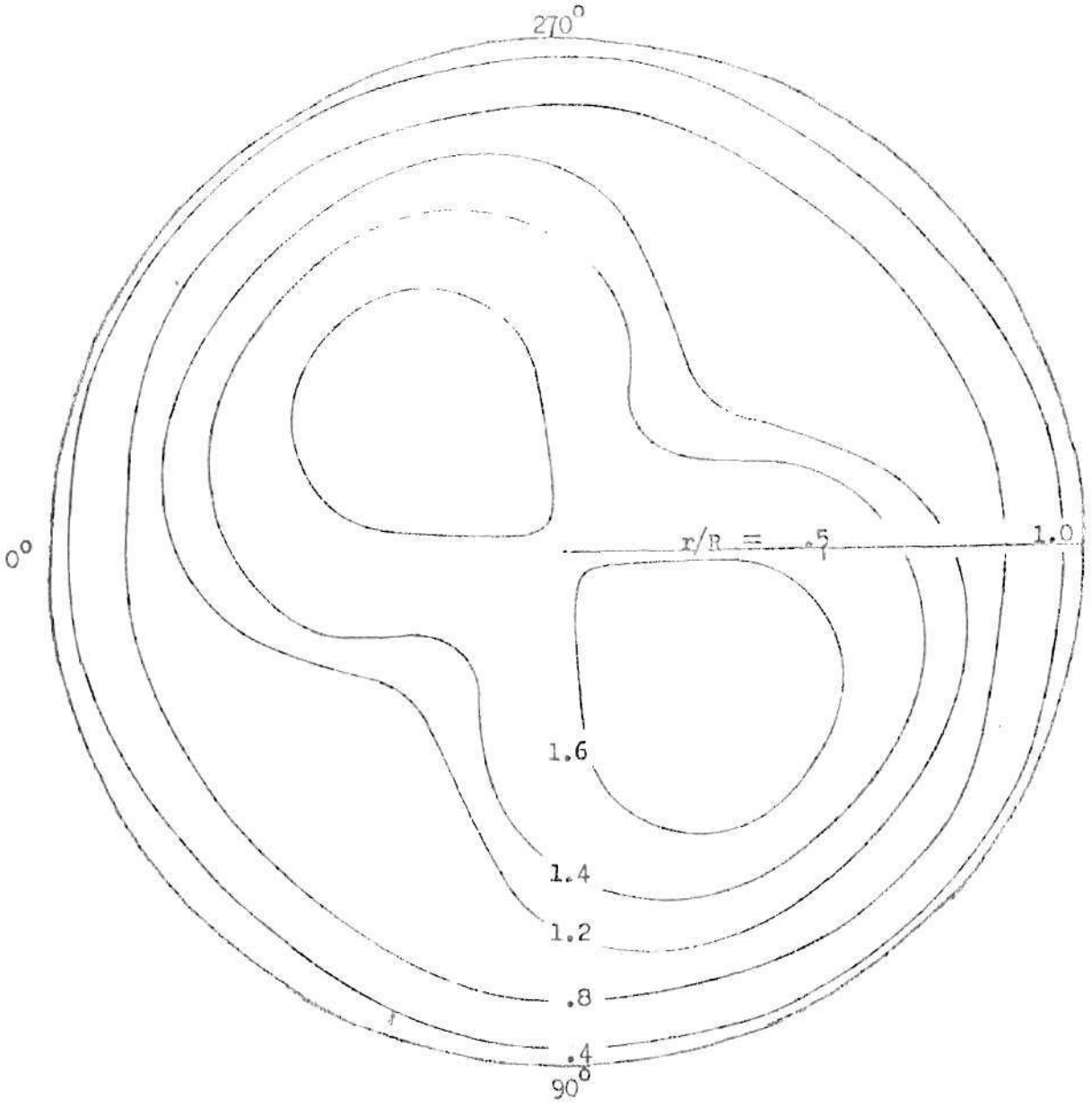


(d) For Nondimensional Distance From Tip Path Plane h/R = 0.2

Figure 7. Continued

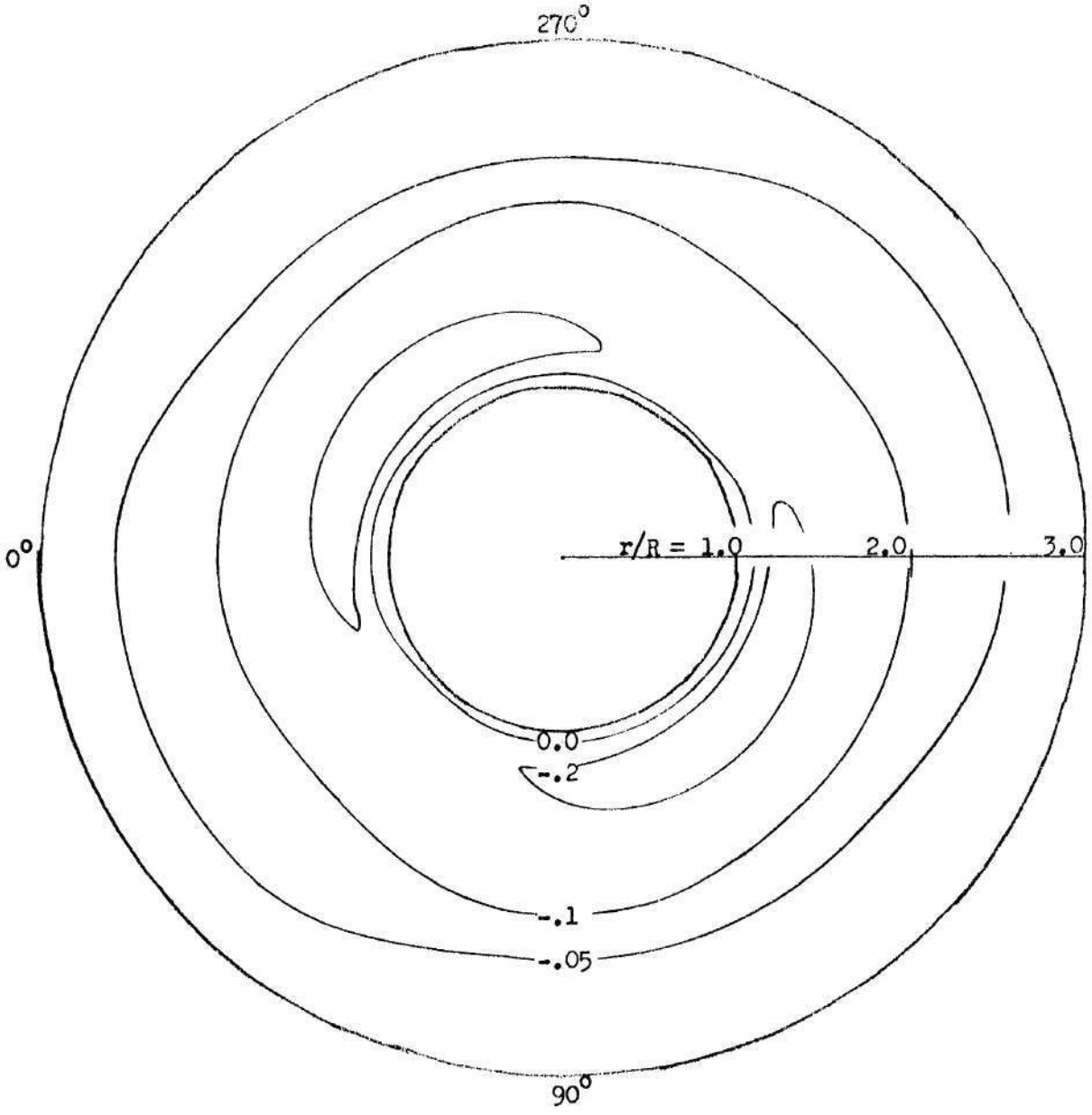


Figure 7(d). Continued

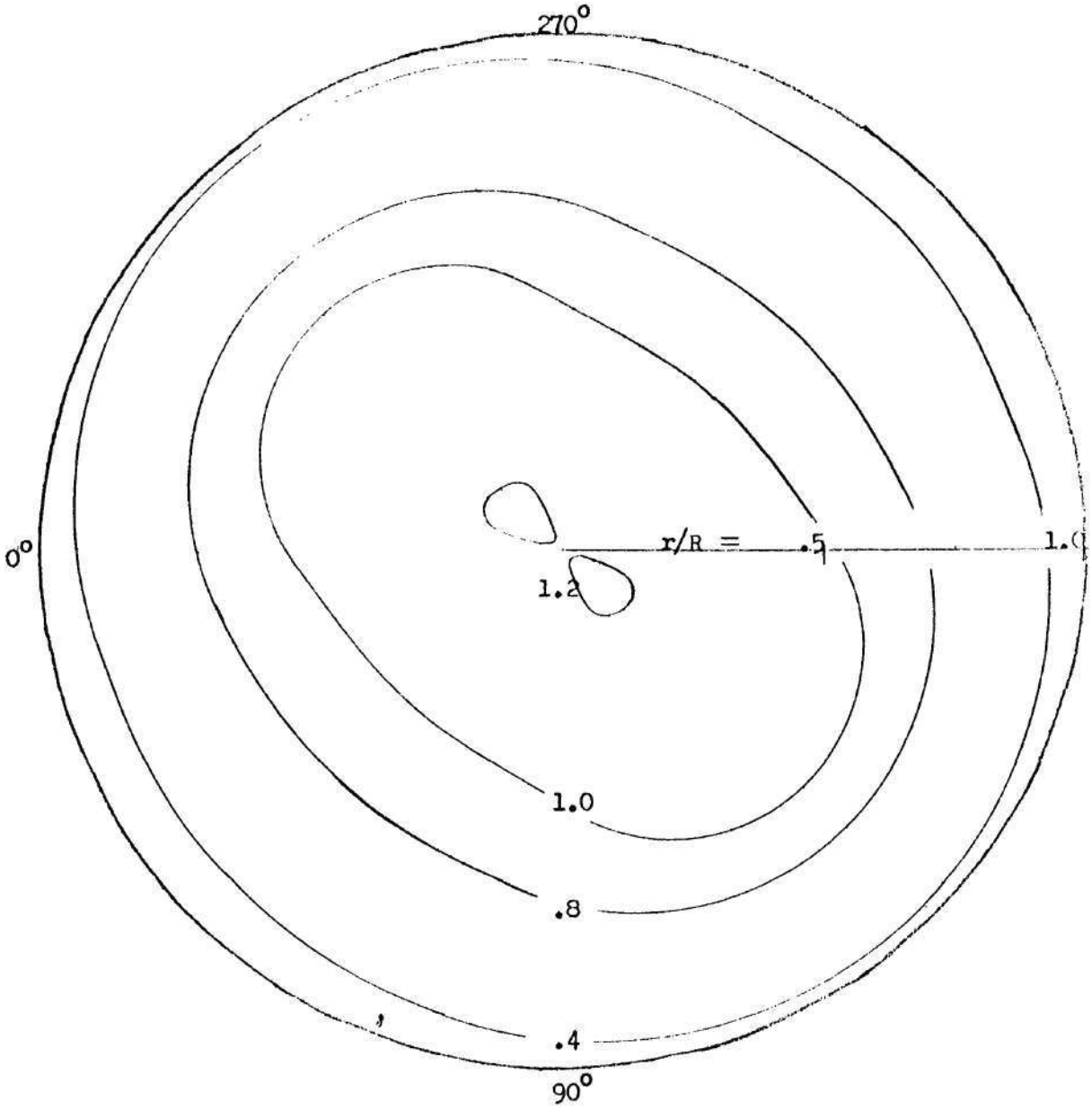


(e) For Nondimensional Distance From Tip Path Plane h/R = 0.4

Figure 7. Continued

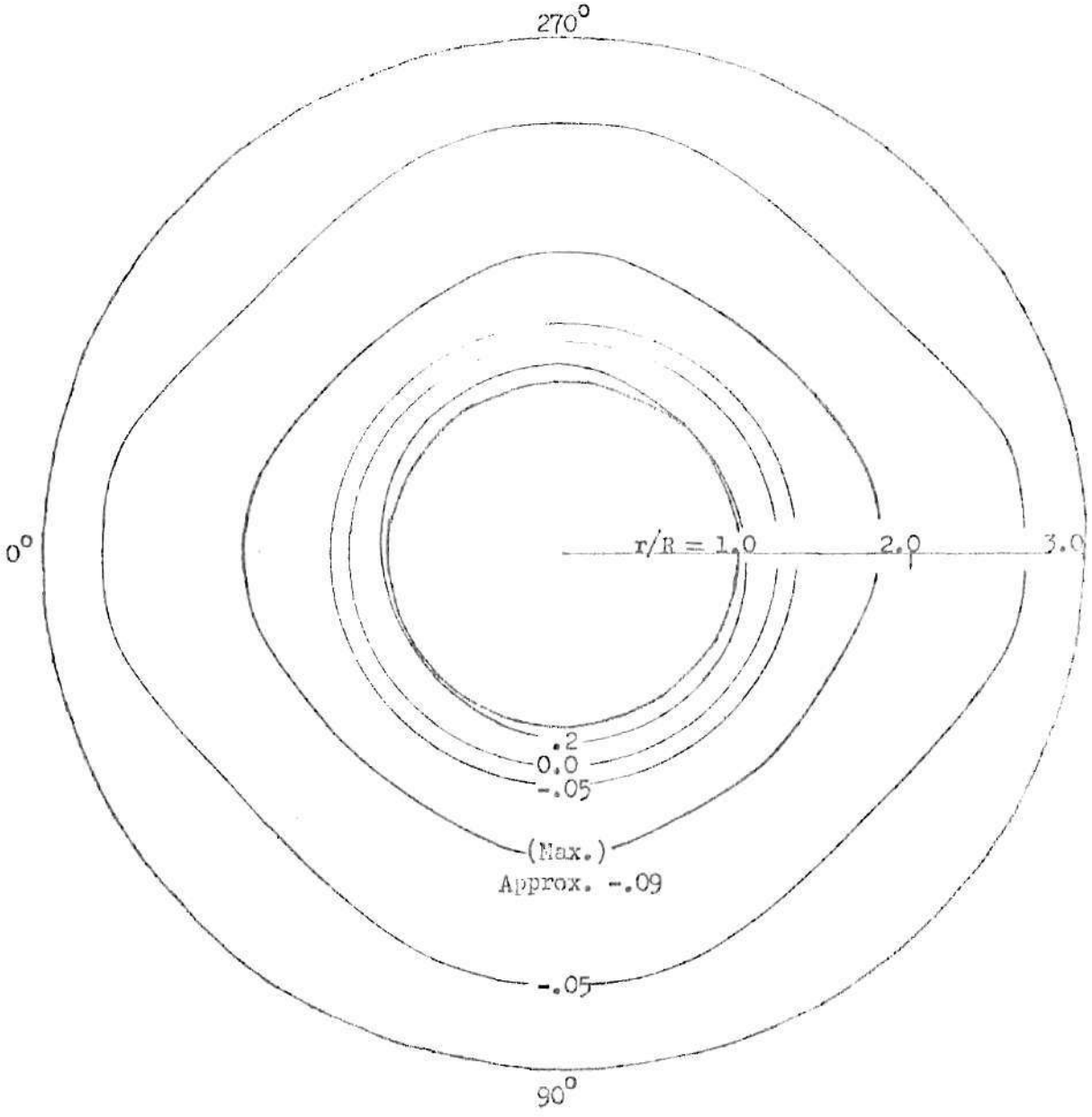


Figure 7(e). Continued

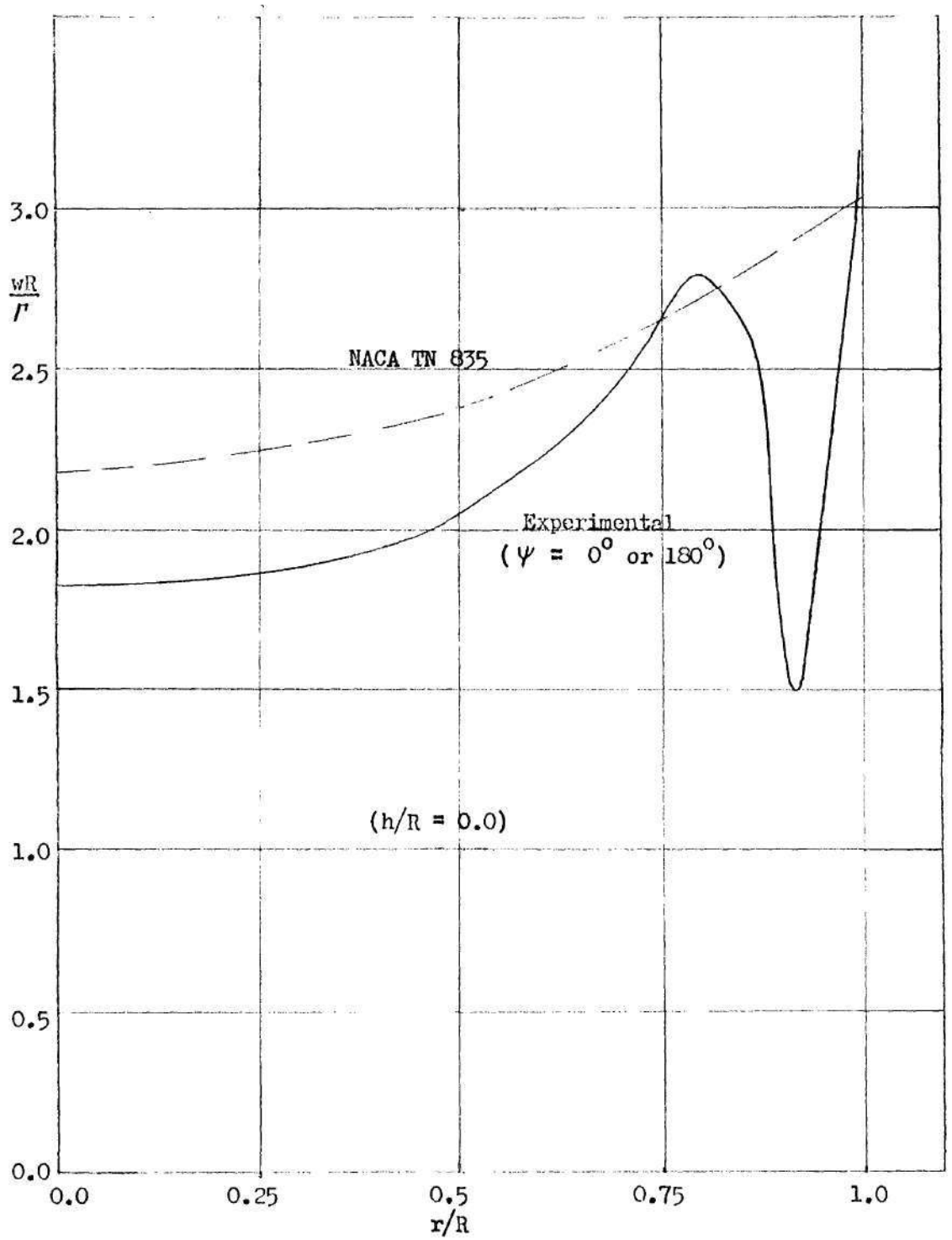


Figure 8. Comparison of Experimental Data With That From NACA TN 835

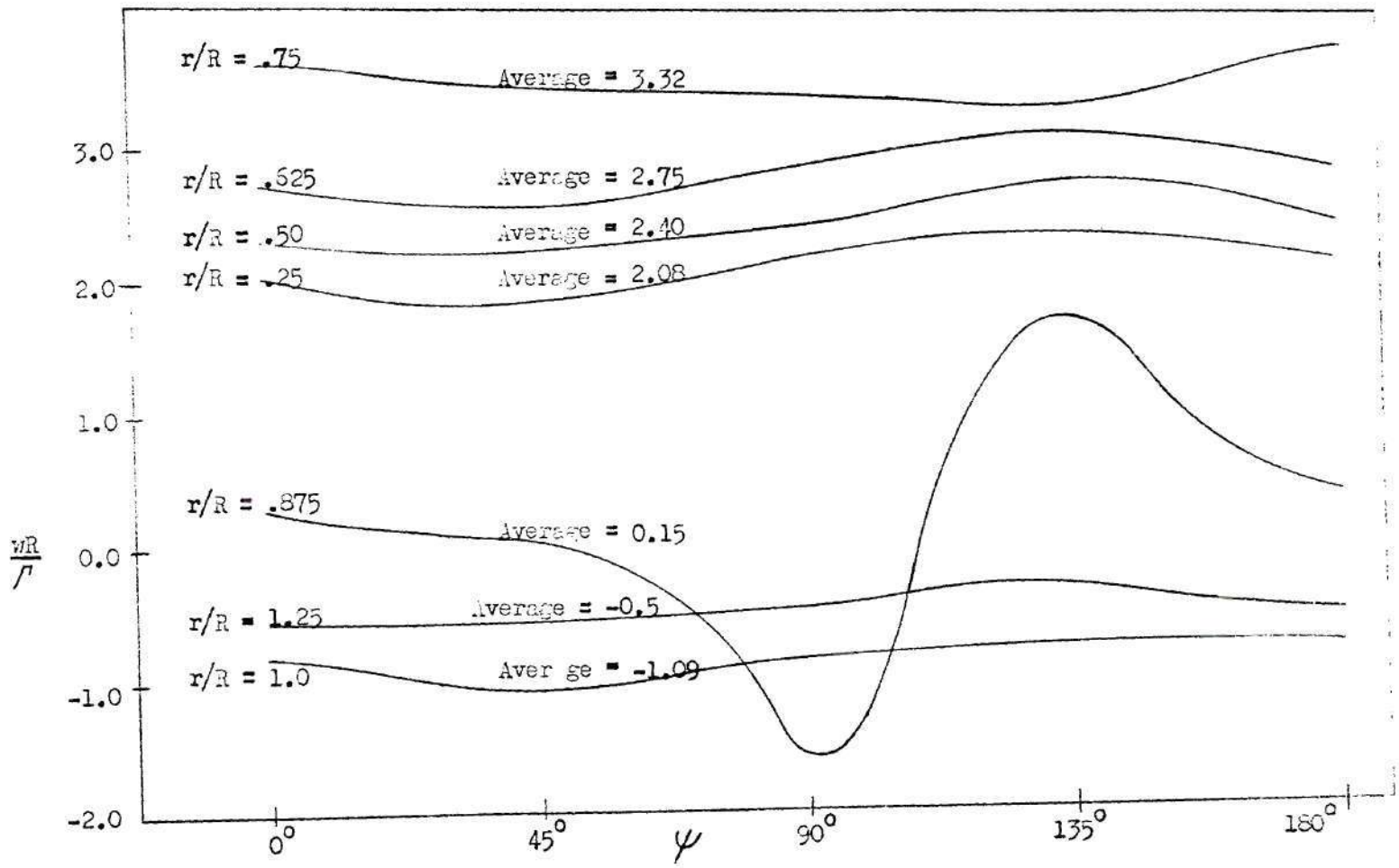


Figure 9. Variation of Nondimensional Normal Component of Induced Velocity With Azimuth Angle Illustrating the Determination of Mean Values

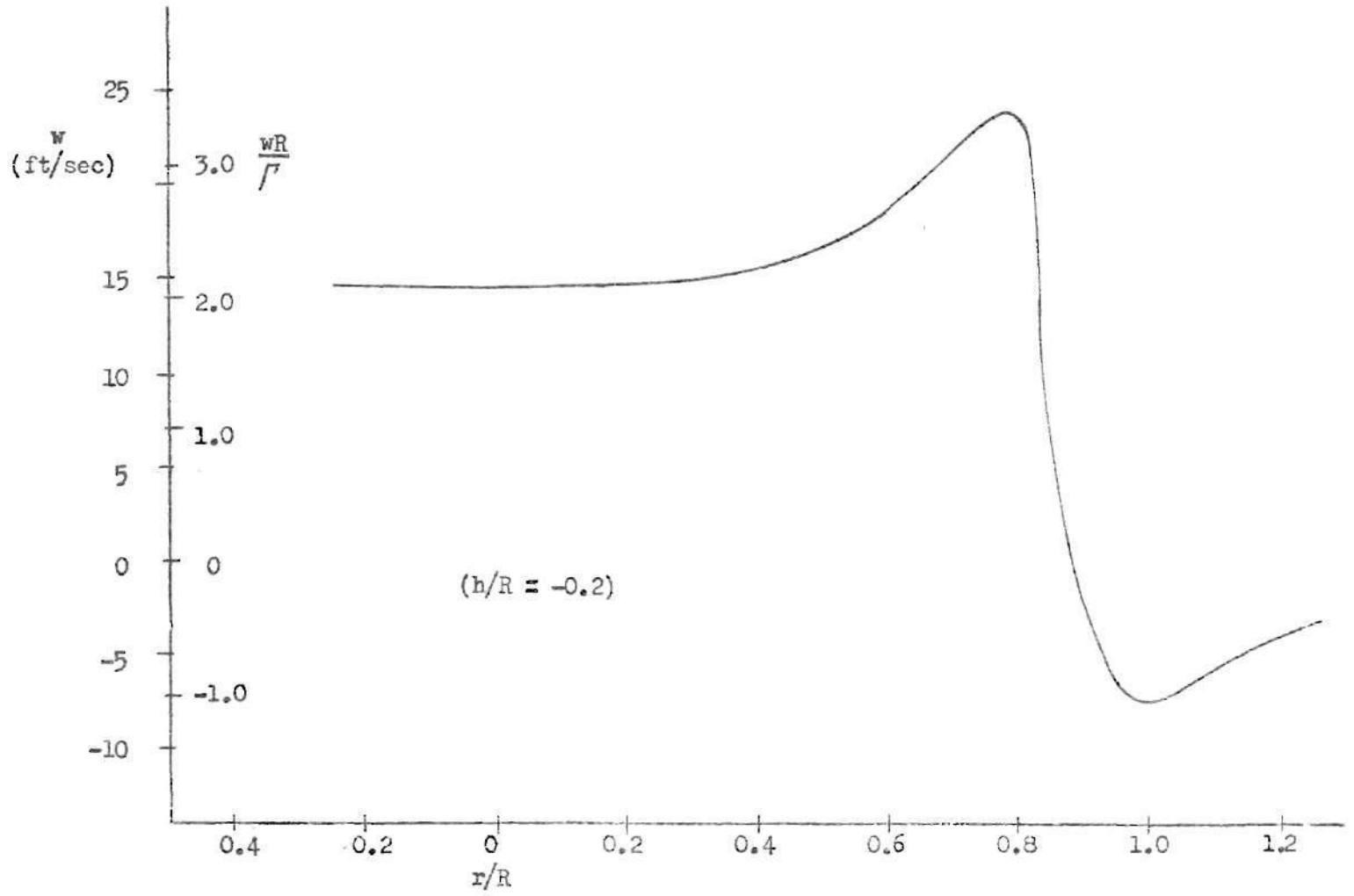


Figure 10. Variation of Mean Downwash Velocity With Distance From the Rotor Axis as Estimated in a Sample Problem

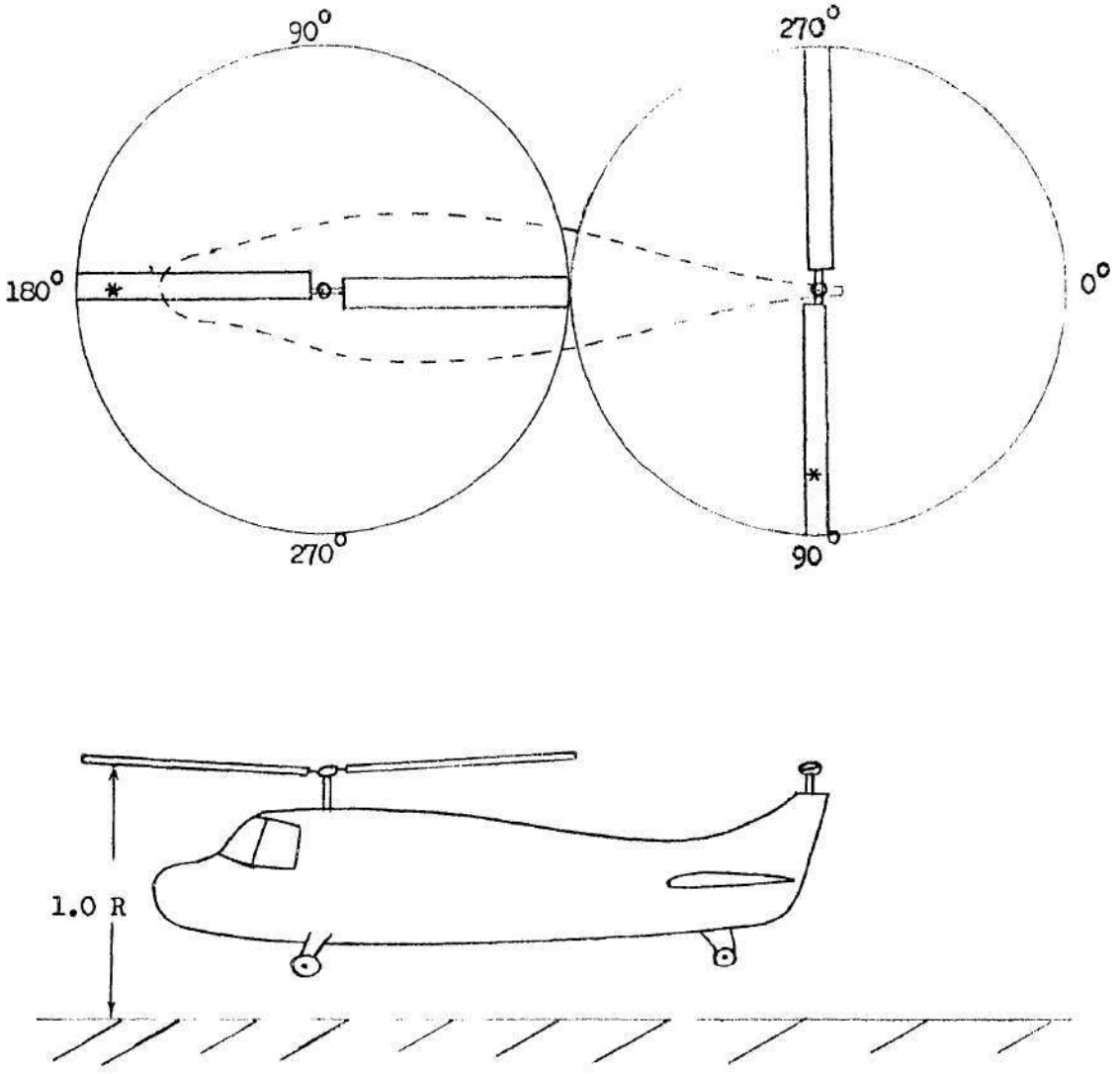


Figure 11. General Configuration of Typical Tandem-Rotor Helicopter Used in a Sample Problem

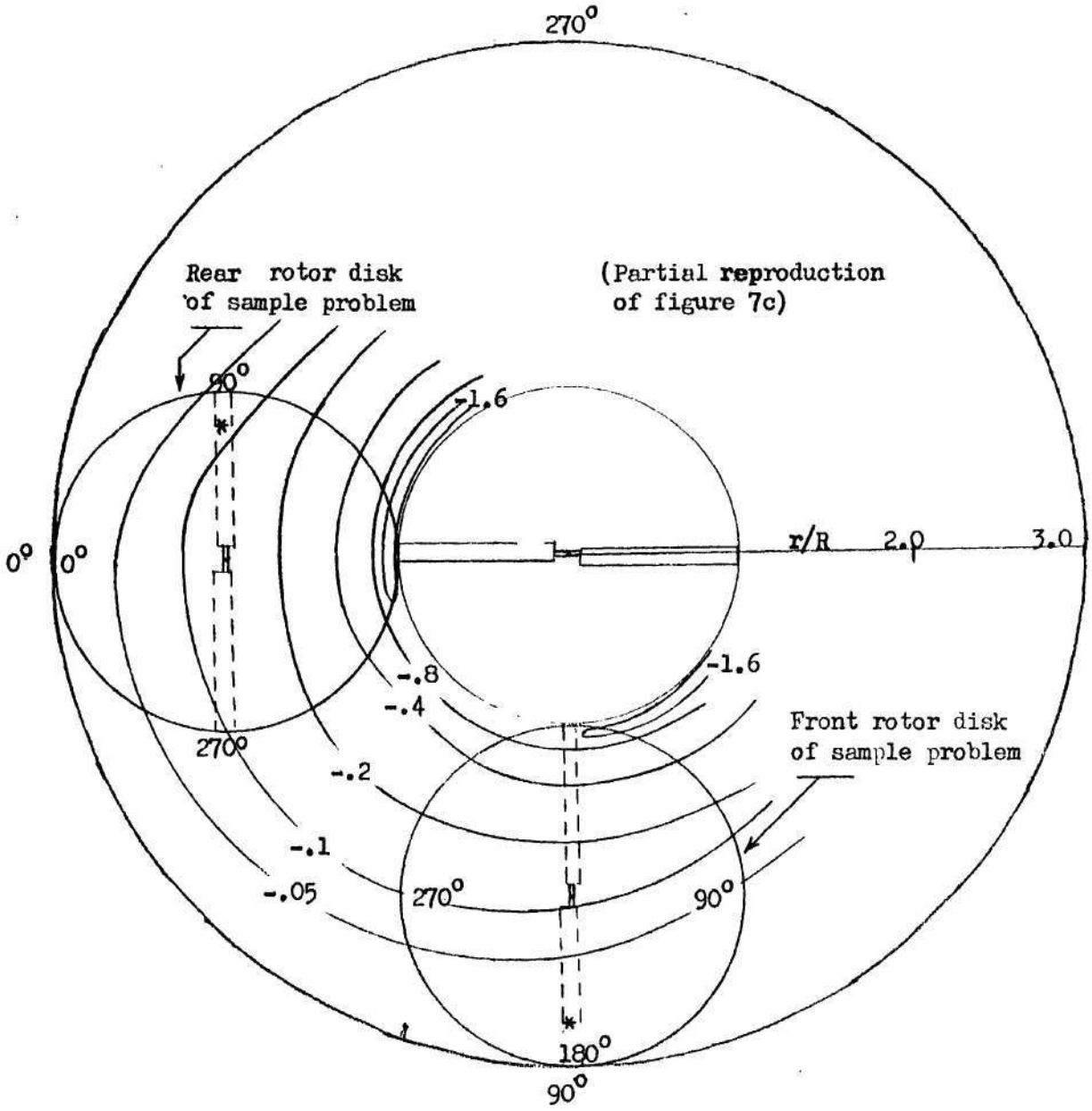


Figure 12. Determination of Interference Nondimensional Component of Induced Velocity For a Sample Problem

# BIBLIOGRAPHY

1. Gray, Robin B., An Experimental Smoke and Magnetic Analogy Study of the Induced Flow Field About a Model Rotor in Steady Flight Within Ground Effect, National Aeronautics and Space Administration, Contract NAw 6520, August, 1959.

2. Castles, Walter, Jr., Howard L. Durham, Jr., and Jiriar Kevorkian, Normal Component of Induced Velocity For Entire Field of a Uniformly Loaded Lifting Rotor With Highly Swept Wake As Determined By Electromagnetic Analog, National Aeronautics and Space Administration, Technical Note 4238, 1958.

3. Knight, Montgomery and Ralph A. Hefner, Analysis of Ground Effect On the Lifting Airscrew, National Advisory Committee for Aeronautics, Technical Note No. 835, 1941.